Real-time single-molecule imaging of oxidation catalysis at a liquid–solid interface

BAS HULSKEN[1], RICHARD VAN HAMEREN[2], JAN W. GERRITSEN[1], TONY KHOURY[3], PALL THORDARSON[2,3], MAXWELL J. CROSSLEY[3], ALAN E. ROWAN[4], ROELAND J. M. NOLTE[2], JOHANNES A. A. W. ELEMANS[1,2]* AND SYLVIA SPELLER[1]

[1]Scanning Probe Microscopy, Institute for Molecules and Materials, Radboud University Nijmegen, Toernooiveld 1, 6525 ED, Nijmegen, The Netherlands
[2]Physical Organic and Supramolecular Chemistry, Institute for Molecules and Materials, Radboud University Nijmegen, Toernooiveld 1, 6525 ED, Nijmegen, The Netherlands
[3]School of Chemistry, The University of Sydney, Sydney, NSW 2006, Australia
[4]Molecular Materials, Institute for Molecules and Materials, Radboud University Nijmegen, Toernooiveld 1, 6525 ED, Nijmegen, The Netherlands
*e-mail: j.elemans@science.ru.nl

Published online: 22 April 2007; doi:10.1038/nnano.2007.106

Many chemical reactions are catalysed by metal complexes, and insight into their mechanisms is essential for the design of future catalysts. A variety of conventional spectroscopic techniques are available for the study of reaction mechanisms at the ensemble level, and, only recently, fluorescence microscopy techniques have been applied to monitor single chemical reactions carried out on crystal faces[1] and by enzymes[2–4]. With scanning tunnelling microscopy (STM) it has become possible to obtain, during chemical reactions, spatial information at the atomic level[5–9]. The majority of these STM studies have been carried out under ultrahigh vacuum, far removed from conditions encountered in laboratory processes. Here we report the single-molecule imaging of oxidation catalysis by monitoring, with STM, individual manganese porphyrin catalysts, in real time, at a liquid–solid interface. It is found that the oxygen atoms from an O_2 molecule are bound to adjacent porphyrin catalysts on the surface before their incorporation into an alkene substrate.

Metal-porphyrins are dyes that occur in nature, where they are involved in processes such as light harvesting in plants and oxygen binding in haem. Synthetic Mn(III) porphyrins are often used as catalysts for the chemical transformation of alkenes into epoxides, in which an oxygen atom is added across a carbon–carbon double bond to form a three-membered ring[10]. Generally, the porphyrins activate an external oxidant, such as a peroxide or hypochlorite, by binding its oxygen atom to their metal centre, allowing its subsequent transfer to an alkene to yield an epoxide or other oxidized product. As in the case of the naturally occurring mono-oxygenase enzyme cytochrome P450 (refs 11 and 12), molecular oxygen can be used as an oxidant, although in this case additional electrons are required to facilitate oxygen–oxygen bond cleavage in a process known as reductive activation. We reason that a metal surface could also function to activate a catalyst to react with molecular oxygen, and have used the flat manganese porphyrin **Mn1** as an epoxidation catalyst (Fig. 1a).

Initially, the ability of **Mn1** to form self-assembled monolayers at the interface of a Au(111) surface and an argon-saturated *n*-tetradecane liquid phase[13] was investigated in a liquid-cell STM equipped with a bell jar containing an argon atmosphere. Upon the addition of **Mn1** to the solution ($[\mathbf{Mn1}] = 10^{-8}$ M), the formation of extended monolayer domains at the liquid–solid interface, with the porphyrins adsorbed face-on to the surface in regular patterns, was observed (Fig. 1b, c). Ultraviolet-visible (UV-vis) reflection measurements of this monolayer suggested a direct interaction between the porphyrins and the Au(111) surface, because of an observed 10-nm blue shift from 480 nm to 470 nm of the porphyrin Soret band (a strong absorption band that can provide valuable information about metal-porphyrin redox states) with respect to **Mn1** in tetradecane solution (Fig. 2d). The interaction probably involves a coordination of the metal surface to the manganese centre, because the metal-free derivative of **Mn1** was found not to adsorb to the same interface[14].

The clean and highly defined STM images indicate a nearly uncontaminated interface; however, occasionally, a porphyrin with a much higher apparent height was observed (Fig. 1b). Realizing that manganese porphyrins can react with molecular oxygen[15], a small contamination of the liquid with this gas was suspected. In order to test this hypothesis, the setup was purposely contaminated by flushing the bell jar with O_2. This led to a gradual increase in the number of bright-appearing porphyrins (Fig. 2a), suggesting that these are adsorbed **Mn1** species interacting with oxygen. Concomitant with this change in topography, UV-vis reflection measurements of the interface revealed a red shift of the Soret band from 470 nm to 478 nm (Fig. 2d). The presence or absence of O_2 had no influence on the position of the Soret band of **Mn1** at 480 nm in the UV-vis spectrum in tetradecane solution in the absence of a Au(111) surface. Hence, it is proposed that this surface activates **Mn1** to react with O_2, in a way comparable to an electron-donating axially coordinating ligand[15].

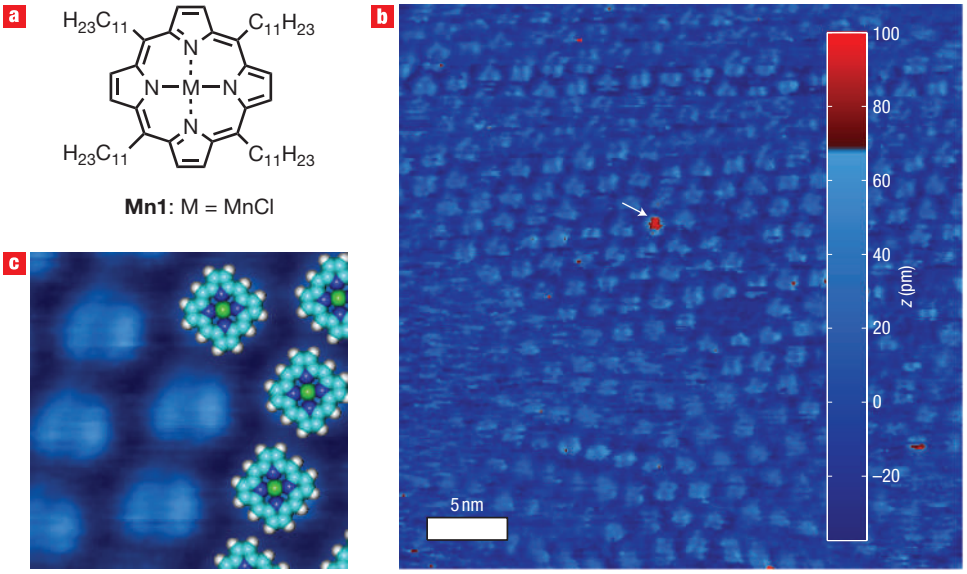

Figure 1 STM studies of manganese porphyrin catalysts. a, Molecular structure of **Mn1**, the porphyrin catalyst, which, for solubility reasons, contains four greasy alkyl chains ($C_{11}H_{23}$). **b**, Liquid-cell STM constant current image ($I = 3$ pA, $V = 200$ mV) of a monolayer of **Mn1** self-assembled at an interface of Au(111) and an argon-saturated *n*-tetradecane liquid phase. Several domains of molecules of **Mn1** are visible. The white arrow indicates a molecule with much higher apparent height. **c**, Correlation averaged enlargement with the suggested molecular orientation drawn in.

To study the nature of the interaction between adsorbed **Mn1** and oxygen in more detail, an investigation was carried out on the distribution of bright-appearing porphyrins in a monolayer of **Mn1** in contact with oxygen. By analysing many locations on the monolayer, it became apparent that the oxygen-containing species primarily occurred in pairs. To quantify this observation, a statistical analysis was carried out on a 75×75 nm area ($\sim$2,000 molecules) of a typical STM image (see Supplementary Information). For a completely random distribution with coverage p, the fraction of oxygen-bound molecules with i oxygen-bound neighbours is expected to follow the equation

$$f_i = \binom{8}{i} p^i (1-p)^{8-i}$$

leading to the left-hand bar diagram in Fig. 2c. Clearly, the experimentally observed distribution of oxygen-containing **Mn1** molecules is not random (see Fig. 2a); in fact, there is a significant preference for pairs of adjacent porphyrins at the cost of monomeric species, suggesting that each molecule of O_2 preferably dissociates upon or after its reaction with **Mn1** at the surface, and forms two identical mono-oxygen-coordinated species. To verify whether this hypothesis can explain the observed distribution of oxygen-containing porphyrins quantitatively, a simulation was carried out, which showed that the calculated distribution of nearest neighbours meets the experimentally observed distribution and not the random one (Fig. 2c; see also Supplementary Information).

The reaction of molecular oxygen with a metallo-porphyrin is well-known from the natural enzyme cytochrome P450 (ref. 11), which contains an Fe(III) protoporphyrin to which an axial ligand is coordinated. After a stepwise two-electron reduction, this complex binds O_2 and cleaves it reductively, leaving one oxygen atom at the porphyrin to produce a reactive high-valent iron-oxo intermediate, and the other one to combine with two protons to produce a molecule of water. In the presence of axially binding ligands, Mn(III) porphyrins in solution can bind and cleave O_2 in a similar manner, after first being reduced by electrons from an added co-reductor[15].

In the liquid-cell STM experiment, however, neither an axial ligand, nor protons, nor an added co-reductor are present. Because binding of O_2 requires reduction of the manganese centre, we propose that the Au(111) surface is responsible for this step, which occurs on adsorption of **Mn1** and is accompanied with the observed blue shift of the Soret band in the UV-vis reflectance spectrum. The Au(111) surface can induce this reduction following two possible mechanisms. The most likely one, and the one proposed here, is that a surface gold atom coordinates to **Mn1** in an axial ligand fashion, allowing a chlorine radical to dissociate[16], thereby reducing the Mn(III) centre to Mn(II) (Fig. 3). A second possibility is that the surface actively reduces **Mn1** through donation of an electron, followed by dissociation of a chloride anion. This mechanism, however, is less likely, because it requires the unfavourable solvation of anions by the apolar solvent, or a reaction of these ions with the negatively biased Au(111) surface.

Because the STM measurements indicate that each reaction with oxygen generates two identical oxidized **Mn1**–oxygen species, we tentatively propose a homolytic dissociation of O_2 and the distribution of both oxygen atoms over two **Mn1** neighbours to generate two reactive Mn(IV)=O species (Fig. 3)[17]. Such a homolytic dissociation has been reported for the oxidation of cyclohexane with a manganese porphyrin catalyst in bulk solution, albeit only under high pressure and at high temperatures[18]. The observed shifts in the UV-vis reflection spectra for both the surface-induced reduction and subsequent oxygen binding of **Mn1** are similar in nature to those observed for analogous reduction and subsequent oxidation of manganese porphyrins in solution, although in the latter case the shifts in wavelength are generally somewhat larger[19].

The oxidized surface can in principle act as a heterogeneous catalyst for epoxidation reactions. To investigate this possibility,

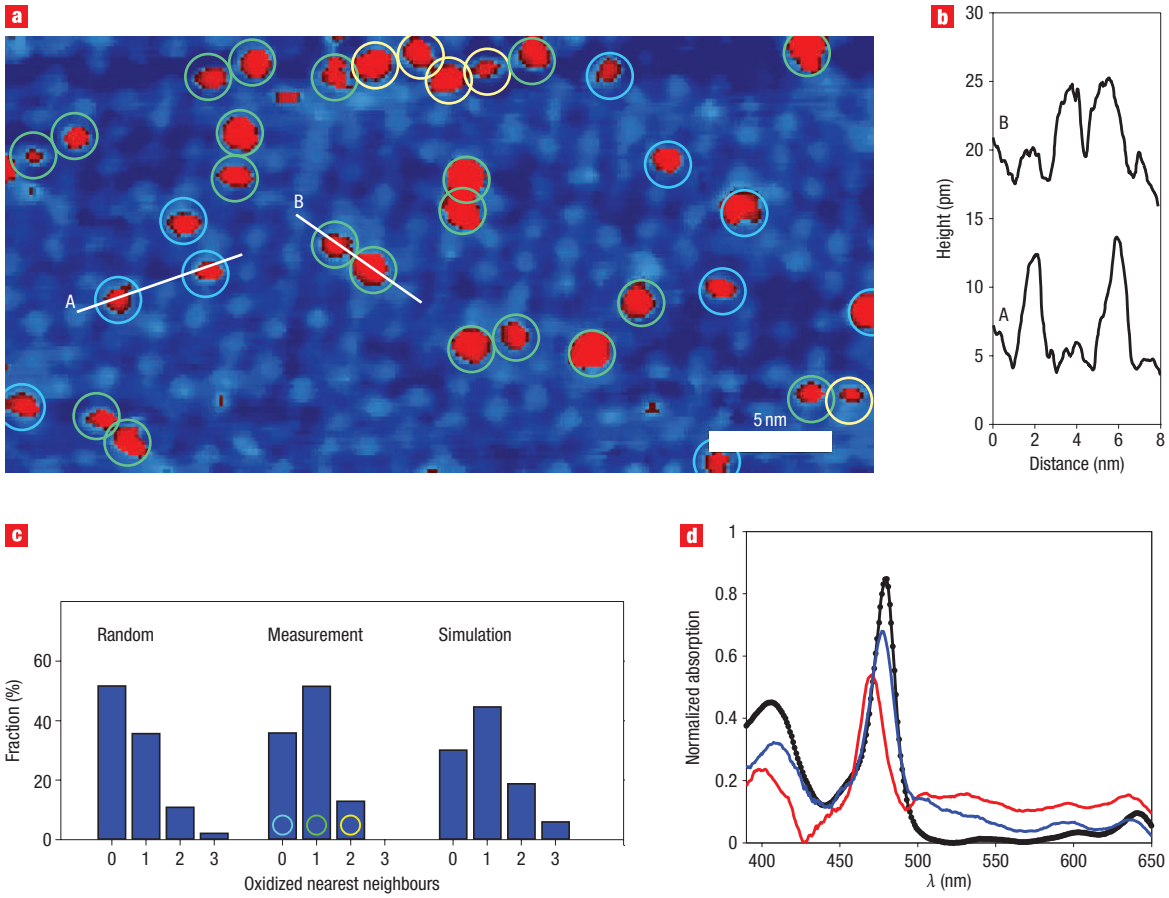

Figure 2 Oxidation of manganese porphyrins at a liquid–solid interface. a, Liquid-cell STM constant current image ($I = 10$ pA, $V = 200$ mV) of a monolayer of **Mn1** self-assembled at an interface of Au(111) and *n*-tetradecane, 4 h after flushing the bell jar with O_2 (overall population of bright spots is ~8%). **b**, Cross-section analyses of the corresponding lines A and B in **a**. **c**, Bar diagrams of nearest-neighbour distributions of oxygen-binding **Mn1** molecules: left, random distribution; middle, distribution as measured in the STM images; right, simulation of a model system (see the text and the Supplementary Information for details). **d**, UV-vis reflectance spectra of a monolayer of **Mn1** at an interface of Au(111) and argon-saturated *n*-tetradecane (red trace), of a monolayer of **Mn1** after oxidation with O_2 (blue trace), and the UV-vis solution spectra of **Mn1** in tetradecane saturated with argon (continuous black trace) and saturated with O_2 (dotted black trace).

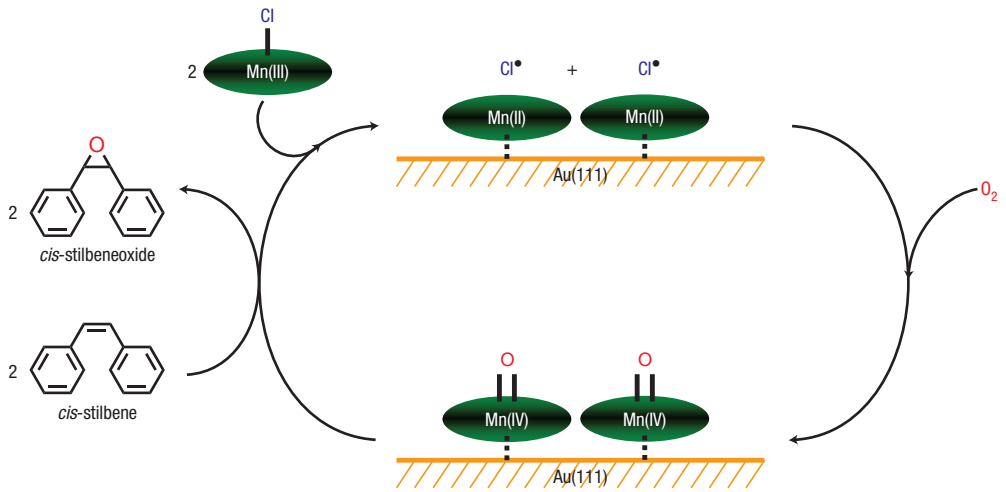

Figure 3 Proposed catalytic cycle of the epoxidation reaction carried out in the liquid-cell STM. Two Mn(III) porphyrins **Mn1** are first attached to the Au(111) surface, which causes their reduction from Mn(III) to Mn(II) with the loss of chlorine radicals. On addition of O_2, two adjacent, identical Mn(IV)-oxo species are formed. These activated species can subsequently insert their oxygen atoms into the double bond of the alkene *cis*-stilbene, resulting in the formation of the epoxide *cis*-stilbeneoxide.

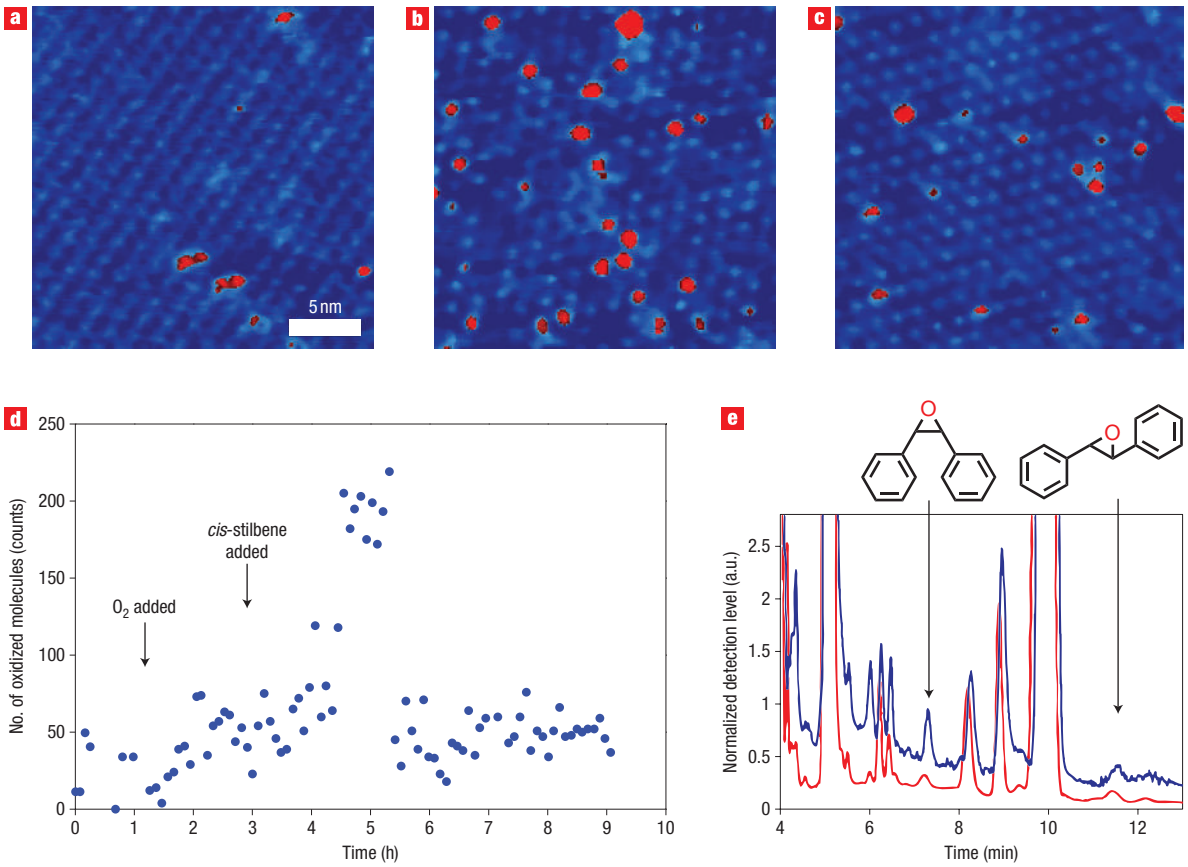

Figure 4 Following the separate steps of a chemical reaction with STM. a–c, Liquid-cell STM constant current images ($I = 10$ pA, $V = 200$ mV) of a monolayer of **Mn1** self-assembled at an interface of Au(111) and *n*-tetradecane. **a**, System under argon. **b**, Four hours after flushing the bell jar with O_2, causing ~10% of the molecules of **Mn1** to be oxidized. **c**, Three hours after the addition of *cis*-stilbene, which has then reached the liquid–solid interface (see Supplementary Information). It is evident that the number of oxidized **Mn1** molecules has decreased significantly. **d**, Plot of the number of oxidized molecules of **Mn1** in a fixed 75 nm × 75 nm area of the surface (~2,000 porphyrins) versus time, on addition of O_2 to the bell jar (at $t = 70$ min) and subsequently the addition of *cis*-stilbene to the top of the liquid in the liquid cell (at $t = 3$ h). **e**, Gas chromatography traces of the tetradecane subphase from the STM cell recorded 19 h (red trace) and 92 h (blue trace) after the addition of *cis*-stilbene; the peaks corresponding to *cis*-stilbene oxide (at time = 7.3 min) and *trans*-stilbene oxide (at time = 11.5 min) are indicated (see also Supplementary Information, Fig. S5).

all the steps of the catalytic epoxidation of *cis*-stilbene (Fig. 3) were followed in real time and real space in the STM liquid-cell setup, by monitoring at a fixed 75 × 75 nm area of the surface (~2,000 porphyrin molecules) the number of oxygen-free and oxygen-binding molecules of **Mn1** (Fig. 4a–d). During the whole experiment, the topography of the surface and the monolayer of **Mn1** remained very stable. While still under an argon atmosphere, the number of oxidized **Mn1** molecules was negligible, but on flushing the bell jar with O_2, their population started to increase rapidly. In order to be able to perform reliable statistical analyses, and because it is known that too high a number of oxidized manganese porphyrin species can lead to catalyst autodestruction[20], at $t = 3$ h, 50 μl of *cis*-stilbene was added very carefully to the surface of the liquid in the STM cell. After ~2.5 h, a period that can correspond well with the expected diffusion time required for the additive to reach the interface (see Supplementary Information), a sudden and significant drop in the number of oxidized **Mn1** molecules was observed, which is proposed to correspond with the start of the oxidation reaction of *cis*-stilbene. In the following four days, the number of oxidized **Mn1** molecules remained at a nearly constant level, which is an indication of long-lasting activity and stability of the surface-bound catalysts.

To verify this assumption, the solution in the liquid-cell STM was analysed by gas chromatography after allowing the reaction to proceed for some time. Although the amount of formed products after almost four days is still very low, the measurement clearly showed a significant increase in concentration of mainly the *cis*-isomer of stilbene oxide (Fig. 4e; see also Supplementary Information, Fig. S5). In the absence of a gold surface, the reaction appeared not to occur.

In conclusion, we have described the first example of real-time single-molecule studies of oxidation catalysis under ambient conditions at a liquid–solid interface. It is evident that the STM approach to studying chemical reactions in a dynamic environment can provide valuable information about reaction mechanisms and rates, as well as catalyst activity and stability. In the present case, this approach has demonstrated a unique aspect about the reaction mechanism, that is, the distribution of both oxygen atoms of O_2 over two adjacent catalysts at the surface, which cannot be measured by conventional ensemble techniques. In addition, by monitoring the single surface-bound

catalysts in real time, it became clear that they remain active and stable for several days.

Received 20 November 2006; accepted 19 March 2007; published 22 April 2007.

References

1. Roeffaers, M. B. J. *et al.* Spatially resolved observation of crystal-face-dependent catalysis by single turnover counting. *Nature* **439,** 572–575 (2006).
2. Lu, H. P., Xu, L. & Xie, X. S. Single-molecule enzymatic dynamics. *Science* **282,** 1877–1882 (1998).
3. Velonia, K. *et al.* Single-enzyme kinetics of CALB-catalyzed hydrolysis. *Angew. Chem. Int. Edn* **44,** 560–564 (2005).
4. Flomenbom, O. *et al.* Stretched exponential decay and correlations in the catalytic activity of fluctuating single lipase molecules. *Proc. Natl Acad. Sci. USA* **102,** 2368–2372 (2005).
5. Hahn, J. R. & Ho, W. Oxidation of a single carbon monoxide molecule manipulated and induced with a scanning tunneling microscope. *Phys. Rev. Lett.* **87,** 166102 (2001).
6. Hendriksen, B. L. M. & Frenken, J. W. M. CO oxidation on Pt(110): Scanning tunneling microscopy inside a high-pressure flow reactor. *Phys. Rev. Lett.* **89,** 046101 (2002).
7. Grim, P. C. M. *et al.* Submolecularly resolved polymerization of diacetylene molecules on the graphite surface observed with scanning tunneling microscopy *Angew. Chem. Int. Edn Engl.* **36,** 2601–2603 (1997).
8. Okawa, Y. & Aono, M. Nanoscale control of chain polymerisation. *Nature* **409,** 683–684 (2001).
9. Hla, S. W., Bartels, L., Meyer, G. & Rieder, K.-H. Inducing all steps of a chemical reaction with the scanning tunneling microscope tip: Towards single molecule engineering. *Phys. Rev. Lett.* **85,** 2777–2780 (2000).
10. Meunier, B. Metalloporphyrins as versatile catalysts for oxidation reactions and oxidative DNA cleavage. *Chem. Rev.* **92,** 1411–1456 (1992).
11. Oritz de Montellano, P. R. (ed.) in *Cytochrome P450: Structure, Mechanism and Biochemistry*, 2nd edn (Plenum Press, New York, 1995).
12. Meunier, B., de Visser, S. P. & Shaik, S. Mechanism of oxidation reactions catalyzed by cytochrome P450 enzyme. *Chem. Rev.* **104,** 3947–3980 (2004).
13. Hulsken, B., Gerritsen, J. W. & Speller, S. Measuring the Au(111) surface state at the solid–liquid interface. *Surf. Sci.* **580,** 95–100 (2005).
14. Hulsken, B. *et al.* Scanning tunneling microscopy and spectroscopy studies of porphyrins at solid-liquid interfaces. *Jap. J. Appl. Phys.* **45,** 1953–1955 (2006).
15. Feiters, M. C., Rowan, A.E. & Nolte, R. J. M. From simple to supramolecular cytochrome P450 mimics. *Chem. Soc. Rev.* **29,** 375–384 (2000).
16. Guo, C.-G. *et al.* Effective catalysis of simple metalloporphyrins for cyclohexane oxidation with air in the absence of additives and solvents. *Appl. Catal. A* **246,** 303–309 (2003).
17. Sheldon, R. A. (ed.) *Metalloporphyrins in Catalytic Oxidations* 267 (Marcel Dekker, New York, Basel, Hong Kong, 1994).
18. Lyons, J. E., Ellis, P. E. & Myers, K. K. Jr. Halogenated metalloporphyrin complexes as catalysts for selective reactions of acyclic alkanes with molecular oxygen. *J. Catal.* **155,** 59–73 (1995).
19. Tabushi, I. Reductive dioxygen activation by use of artificial P450 systems. *Coord. Chem. Rev.* **86,** 1–42 (1988) and references cited therein.
20. Elemans, J. A. A. W., Bijsterveld, E. J. A., Rowan, A. E. & Nolte, R. J. M. Manganese porphyrin hosts as epoxidation catalysts—activity and stability control by axial ligand effects. *Eur. J. Org. Chem.* **2007,** 751 (2007).

Acknowledgements

M. Heijna is acknowledged for assistance with the UV-vis reflectance measurements, and M. C. Feiters for stimulating discussions. The National Research School Combination Catalysis (NRSC-C) (support to R.v.H.) and NanoNed (the Dutch nanotechnology initiative by the Ministry of Economic Affairs) are acknowledged, and the Council for the Chemical Sciences of the Netherlands Organization for Scientific Research (CW-NWO) for financing this research through a Veni innovative research grant to J.A.A.W.E. Correspondence and requests for materials should be addressed to J.A.A.W.E.
Supplementary information accompanies this paper on www.nature.com/naturenanotechnology.

Author contributions

J.A.A.W.E., A.E.R. and R.J.M.N. conceived and designed the epoxidation experiment. S.S. and J.A.A.W.E. were responsible for the STM experiment. B.H. and R.v.H. carried out the experiments. J.W.G. supplied technical support. T.K., P.T. and M.J.C. designed and synthesized the particular porphyrin catalyst. All authors discussed the results and commented on the manuscript.

Competing financial interests

The authors declare that they have no competing financial interests.